

Phase-Space Bounds on the Mass of Dark Matter in Fermi Degenerate Non-Isothermal Galaxies

Ahmad Borzou

EUCOS-CASPER, Physics Department, Baylor University, Waco, TX 76798-7316, USA

Abstract

The phase-space bounds on the mass of dark matter are mostly derived for isothermal galactic halos. In this paper, we study slight deviations from the isothermal condition. We show that if fermionic dark matter in galaxies has a Maxwellian distribution, small variations in the temperature of dark matter are negligible. However, in highly Fermi degenerate halos, diversions from constant temperature are multiplied by the infinite Fermi-Dirac integrals and can be significant. We develop computer software to study non-isothermal effects in the full range of classical to highly degenerate dark matter halos. Using the data of the Fornax dwarf galaxy, we show that with a temperature gradient of not more than 0.002 Kelvin per kiloparsec, it is possible to compress fermionic dark matter with the mass of 2 eV into a radius less than 1 kiloparsec and build a halo with the total mass of $\sim 10^8$ of the mass of the sun.

Keywords: Dark matter, elementary particles, Neutrino, dwarf

Email address: ahmad_borzou@baylor.edu (Ahmad Borzou)

1. Introduction

A variety of independent observations leave no doubt on the existence of dark matter (DM). These include the early measurements of galaxies velocity dispersion in the Coma cluster [1], the rotation curves in galaxies [2], the recent measurements of the gravitational lensing [3, 4], the Bullet cluster [5], the anisotropies in the CMB [6], and the large scale structures [7].

No candidate particle is observed in any of the experimental searches [8, 9, 10, 11]. The only stable and invisible particles that have been observed are active neutrinos. Nevertheless, there are two obstacles against their candidacy for DM. The standard model (SM) predicts that neutrinos freeze-out relativistically in the early universe. This, on the other hand, contradicts the large scale structure observations that are in favor of a non-relativistic freeze-out. However, the relativistic freeze-out of neutrinos is not observationally confirmed and is solely a prediction of SM. On the other hand, the neutrino sector of SM is the least understood part of the theory, and its predictions are already at odds with observations [12]. It is, therefore, legitimate to question the validity of this prediction. As is shown in [13] and will be briefly discussed below, there is still a wide range of neutrino models that are allowed by observations in which neutrinos freeze-out non-relativistically in the early universe. In these scenarios, a negligible interaction keeps neutrinos in thermal contact until the temperature of the universe falls below their mass. It is interesting to note that the small scale crisis of the cold dark matter (CDM) model, has already motivated a wide range of self-interacting dark matter (SIDM) which has received high attention from the community [14, 15].

Another limitation against the DM candidacy of active neutrinos originates from their fermionic nature. These bounds are derived by (I) assuming a phase-space distribution for DM in galaxies, (II) solving the hydrostatic equilibrium to fix the parameters of the assumed distribution, (III) compare the maximum of the distribution with the maximum allowed by the Fermi-Dirac distribution to find a lower limit on the mass of the fermionic DM. The lower limits on the mass of fermionic dark matter are usually above 1 keV if the assumed distribution is Maxwell-Boltzmann [16, 17]. Motivated by the core-cusp problem of CDM, these limitations are recently re-considered for highly degenerate isothermal DM halos where the lower bounds are shifted down to ~ 100 eV [18, 19]. In the following, we discuss that a constant temperature across DM halos is not validated through observations. Moreover, even for collision-less DM models, there are a variety of heat generation mechanisms that can lead to at least slight deviations from isothermal models. In highly Fermi degenerate halos, these deviations will be amplified by infinite Fermi-Dirac integrals and become significant. We show that a slight temperature gradient in the high degeneracy regime substantially lowers the phase-space bounds on the mass of DM. It is important to note that regardless of the temperature of dark matter, there is always an upper DM mass below which the dark halo is degenerate. Therefore, the degeneracy condition will be satisfied precisely at the DM mass range that the so-called phase-space bounds are trying to rule out.

In this paper, we derive the most general hydrostatic equilibrium equation for a spherical Fermi-Dirac DM distribution. Computer software is developed to solve the field equations numerically. We validate the software

by reproducing the classic isothermal exact solution of the hydrostatic equilibrium and the numeric solutions for fully degenerate isothermal DM. Since the analysis is meant to be general, rather than assuming a specific DM and galactic model in order to derive an equation for temperature gradient, we reserve the assumption for directly inserting a temperature profile into the software.

After assuming a linear temperature gradient, we use an optimization method to determine its single free parameter using the data for the dispersion velocity of the visible matter in the Fornax dwarf satellite galaxy of the Milky Way. The solution is then compared with an isothermal but otherwise identical system. We show that for a DM mass of 2 eV, the isothermal solution extends to around 500 kiloparsecs (kpc) while the non-isothermal solution has a radius of less than 1 kpc with a temperature gradient of not more than 0.002 Kelvin per kpc.

We also review the gravitational and non-gravitational frictions and gravitational contraction as the sources of heat generation and radiation and convection as the means of heat transfer in DM halos. The frictional effects may play crucial roles in satellite galaxies that move with relatively high speeds through their host galaxies.

This paper is organized as follows. In section 2, we discuss the possibility of cold active neutrino DM. Section 3 is devoted to a brief review of the Fermi-Dirac statistics. In section 4, the equilibrium equations are derived. The computer software for solving the equations is discussed. In section 5, we first validate the software by reproducing two known solutions of the equilibrium equations. Next, we discuss the phase-space bounds on the mass

of DM. Finally, non-isothermal solutions are studied. Section 6 is devoted to the sources of heat generation and the means of heat transfer in galaxies. A conclusion will be drawn in section 7.

2. Cold active neutrino DM

Observations of the large scale structures in the universe are in favor of a cold DM [20, 21]. On the other hand, SM predicts that neutrinos are hot. Nevertheless, some of the predictions of the neutrino sector of SM are not consistent with observations [12], and models of neutrinos are still being investigated today. More importantly, the hotness of active neutrinos has not been confirmed experimentally.

In this section, we would like to examine the possibility of introducing a weak long-range interaction between neutrinos such that they freeze-out cold in the early universe. The bounds on such interaction are the strongest if it acts on the charged leptons as well. In this case, the interaction contributes to the anomalous magnetic moment of electrons as the most precisely tested variable in physics. The standard model prediction for it can be found in [22], and the experimentally measured value can be found in [23]. The two are in agreement in eleven significant digits. If the proposed interaction is QED-like, its correction to the anomalous magnetic moment is $\frac{\alpha'}{8\pi^2}$ where α' is the corresponding fine structure. The anomalous magnetic moment leaves an upper bound of roughly $\alpha' < 10^{-10}$ on the fine structure of the dark interaction. It should be noted that the bound will be more relaxed if the interaction solely acts between neutrinos.

At this point, we explore if this weak interaction is strong enough to

delay the neutrino freeze-out until the particles are cold. For a QED-like interaction, the Thomson scattering with a cross-section of $8(\alpha'/m)^2$ is the most effective for our purposes. For neutrinos of mass $m \sim 1$ eV and using the data-driven expansion profile of the universe, one can find that α' has to be larger than 10^{-14} to delay the freeze-out of neutrinos until they are cold. The bound is even lower for lighter particles. A detailed derivation of this bound can be found in [13]. From the considerations above, we see that there is still a wide range of unexplored phase-space, $10^{-14} < \alpha' < 10^{-10}$, in which neutrinos can freeze-out non-relativistically in the early universe.

It is interesting to note that the small scale problems of CDM have motivated a class of by now prevalent SIDM with relativistic force carriers which are quite similar to our proposed scenario for active neutrinos. See for example [24]. The interaction between neutrinos not only helps to surpass the cosmological limitations of neutrino DM but also can be used to establish a temperature gradient in the DM halo which, as we will see later in this paper, is needed to surpass the so-called phase-space bounds. Nevertheless, we would like to emphasize that the phase-space analysis presented in the following is independent of interacting neutrinos and can be applied to any class of DM with any DM mass.

3. An overview of Fermi-Dirac statistics

In this section, we derive the equation of state (EOS) of a fermionic DM from its energy-momentum tensor. This approach is particularly advantageous if the corrections to the EOS due to possible interactions between DM

are of interest. The action of a Dirac field reads

$$S = \int d^4x \sqrt{-g} \bar{\psi} \left(\frac{i}{2} \gamma^i e_i^\mu D_\mu - \frac{i}{2} \overleftarrow{D}_\mu \gamma^i e_i^\mu - m \right) \psi, \quad (1)$$

where g is the determinant of the metric, e is the tetrad, m is the mass of DM, and D is the covariant derivative. Since potential interactions have negligible effect on the EOS, we ignore them in this paper and replace $D_\mu \rightarrow \partial_\mu$. The energy-momentum tensor can be found from the action using its invariance under translations

$$\begin{aligned} T^{\alpha\beta} &= \frac{\delta \mathcal{L}}{\delta e_{i\alpha}} e_i^\beta + g^{\alpha\beta} \mathcal{L} \\ &= \frac{i}{2} \bar{\psi} \left(\gamma^i e_i^\alpha \partial^\beta - \overleftarrow{\partial}_\beta \gamma^i e_i^\alpha \right) \psi + g^{\alpha\beta} \mathcal{L}. \end{aligned} \quad (2)$$

The energy density and the pressure of the system are the temporal and the spatial components of the energy-momentum tensor respectively

$$\begin{aligned} \rho_{\text{energy}} &= \frac{1}{V} \int d^3x T_0^0, \\ P &= \frac{1}{3} \int d^3x (T_1^1 + T_2^2 + T_3^3), \end{aligned} \quad (3)$$

where the integral is over microscopic scales and V is a local volume.

The equilibrium equations can be equivalently derived in the lab or free-falling frames. In the lab frame, one needs to use the weak field approximations to write the metric as $g_{\mu\nu} = (1 - 2\Phi, -1, -1, -1)$ where Φ satisfies the Poisson equation. The correction to the metric enters the distribution function of fermions through Eq. (2). A derivative of Eq. (3) with respect to a global length leads to the equation for hydrostatic equilibrium. The disadvantages of this approach are that the equations contain both astronomical and microscopic lengths, the equations are not manifestly covariant anymore,

and cumbersome calculations are needed in the case of strong gravitational effects.

In a free-falling frame, the gravitational effects are absent, and the metric in Eq. (3) is Minkowskian. Working in this frame, we insert the free field expansion of the fermionic field

$$\psi(x) = \sum_{k,\sigma} \left(\frac{m}{V\varepsilon_k} \right)^{\frac{1}{2}} c_k^\sigma u^\sigma(k) e^{-ik \cdot x}, \quad (4)$$

where the sum is over momentum and spin states respectively, ε_k is the energy of each state, c_k^σ is the fermionic operator, and $u^\sigma(k)$ is the free fermionic spinor. After inserting this expansion into Eq. (3), the energy density and pressure read

$$\begin{aligned} \rho_{\text{energy}} &= \frac{1}{V} \sum_{k\sigma} \varepsilon_k c_k^{\dagger\sigma} c_k^\sigma, \\ P &= \frac{1}{3V} \sum_{k\sigma} \frac{\varepsilon_k^2 - m^2}{\varepsilon_k} c_k^{\dagger\sigma} c_k^\sigma. \end{aligned} \quad (5)$$

Since $c_k^{\dagger\sigma} c_k^\sigma$ is the number operator, the number density can be written as

$$n = \frac{1}{V} \sum_{k\sigma} c_k^{\dagger\sigma} c_k^\sigma. \quad (6)$$

The observable quantities are the ensemble average of the corresponding quantum operators and the ensemble average of the number operator reads

$$\langle c_k^{\dagger\sigma} c_k^\sigma \rangle = \frac{1}{z^{-1} e^{\beta\varepsilon_k} + 1}, \quad (7)$$

where z is the fugacity, and $\beta = \frac{1}{kT}$ is the inverse of the Boltzmann constant times the temperature. At this point we make the following replacement

$$\frac{1}{V} \sum_{k\sigma} \rightarrow \frac{1}{\pi^2} \int_m^\infty \varepsilon \sqrt{\varepsilon^2 - m^2} d\varepsilon, \quad (8)$$

and define $\alpha \equiv \frac{h}{\sqrt{2\pi m}}$ in terms of the Planck constant. Using the non-relativistic approximation $\varepsilon \simeq m + \frac{p^2}{2m}$, and inserting Eq. (7) into Eq. (5), the pressure, the energy density, and the mass density defined as $\rho \equiv mn$ read

$$\begin{aligned} P &= \frac{2(kT)^{\frac{5}{2}}}{\alpha^3} f_{\frac{5}{2}}(z), \\ \rho_{\text{energy}} &= \frac{3}{2}P, \\ \rho &= \frac{2m(kT)^{\frac{3}{2}}}{\alpha^3} f_{\frac{3}{2}}(z), \end{aligned} \tag{9}$$

where the Fermi-Dirac integrals are defined as

$$f_{\nu}(z) = \frac{1}{\Gamma(\nu)} \int_0^{\infty} \frac{x^{\nu-1} dx}{z^{-1} e^x + 1}, \tag{10}$$

and $\Gamma(\nu)$ is the gamma function. The equation of state can be easily read from Eq. (9)

$$P = nkTh(z), \tag{11}$$

where

$$h(z) \equiv \frac{f_{\frac{5}{2}}(z)}{f_{\frac{3}{2}}(z)}. \tag{12}$$

When $z \ll 1$, any Fermi-Dirac integral is approximately equal to z and Eq. (11) reduces to the EOS of the classical ideal gas $P = nkT$.

4. Conservation of energy-momentum and stability equations

With a simple transformation, the energy-momentum tensor in the lab frame can be found from the components in the free-falling frame. The

conservation of the energy-momentum tensor together with Newton's field equation leads to the equation for hydrostatic equilibrium

$$\frac{dP}{dr} \simeq -G\rho \frac{M(r)}{r^2}, \quad (13)$$

where G is Newton's constant, and $M(r)$ is the mass enclosed within the distance r . For strong gravitational effects and assuming the validity of the Einstein equation, the conservation law leads to the Tolman-Oppenheimer-Volkoff equation

$$\frac{dP}{dr} = -G(\rho + P) \frac{M(r) + 4\pi r^3 P}{r^2 - 2GM(r)r},$$

which we will not be using in this paper. If DM annihilation and creation are not significant, the conservation of the energy-momentum also implies

$$M(r) = \int_0^r 4\pi r'^2 \rho(r') dr', \quad (14)$$

which is the conservation of mass. The two equations can be combined into a second order differential equation

$$\frac{1}{r^2} \frac{d}{dr} \left(\frac{r^2}{\rho} \frac{dP}{dr} \right) \simeq -4\pi G\rho. \quad (15)$$

Stability equation in dimensionless variables and computer software

Inserting the pressure and mass density from Eq. (9) into Eq. (15), the hydrostatic equilibrium equation reads

$$\frac{1}{\xi^2} \frac{d}{d\xi} \left(\frac{5}{2} \xi^2 h(s) \frac{dy}{d\xi} + \xi^2 y \frac{d(\text{Ln}(s))}{d\xi} \right) = -y^{\frac{3}{2}} f_{\frac{3}{2}}(s), \quad (16)$$

where the dimensionless variables are defined as $\xi \equiv \sqrt{\frac{8\pi G m^2 (kT_0)^{\frac{1}{2}}}{\alpha^3}} r$, $s \equiv \frac{z}{z_0}$, $y \equiv \frac{T}{T_0}$, and naught refers to the values at the center. The boundary

conditions are $s_0 = y_0 = 1$ which are implied by the definitions of s and y and $\frac{ds}{d\xi}|_{\xi=0} = \frac{dy}{d\xi}|_{\xi=0} = 0$ which can be understood from Eq. (13) knowing that $M(r)$ approaches zero faster than r^2 when we move toward the center.

Unfortunately, this equation does not have a known general exact solution, and numerical solutions are of interest. In this paper, we are especially interested in highly degenerate non-isothermal systems in which the fugacity takes values which computers are not able to store, i.e., are computationally infinite. Nevertheless, a close evaluation of Eq. (16) reveals that in the case of high degeneracy, the equation can be entirely expanded in terms of the natural logarithm of the fugacity. Because, except the derivative of $\text{Ln}(s)$ which is already in the desired form, the rest of the dependences on the fugacity are through the Fermi-Dirac integrals that for $\text{Ln}(s) \gg 1$ can be expanded using the Sommerfeld approximation

$$f_\nu(z) = \frac{(\text{Ln}(z))^\nu}{\Gamma(\nu + 1)} \left(1 + \frac{\pi^2 \nu (\nu - 1)}{6} (\text{Ln}(z))^{-2} + \dots \right). \quad (17)$$

On the other hand, in the classical limits, the logarithm can be converted into the fugacity with no difficulty. Therefore, numerical solutions of the differential equation are sought in terms of y and $\text{Ln}(s)$.

A computer program is developed to study galaxies at any temperature and fugacity [25]. The mass of DM, the central values for the number density and the temperature, and the second derivative of the dimensionless temperature with respect to ξ are taken from the user as inputs. The latter is to preserve the generality of the software and allows linking the program to data-driven optimization methods for phenomenological investigation of galactic temperatures. The reason for this approach is that, as we will see in section 6, the equation for temperature gradient not only depends on the

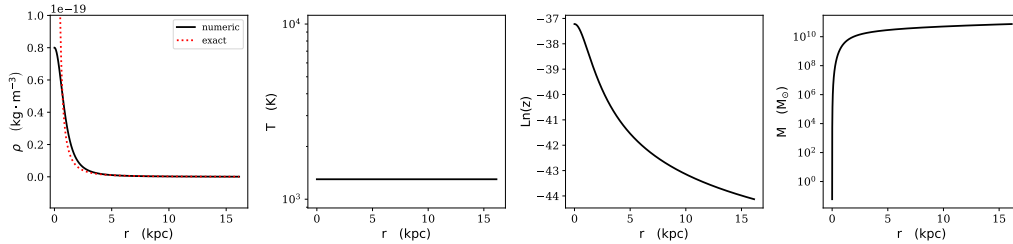


Figure 1: A classic isothermal galaxy with DM mass of 1 MeV and temperature of 1300 Kelvin. The red dashed line indicates the exact solution which suffers from a singularity at the center. The initial conditions are set at the distance of 1 pc from the center to avoid the singularity.

DM model but also is a function of the environmental variables of a specific galaxy.

The software starts from the center of the galaxy and moves toward the edge in the steps of a tenth of a parsec (pc) until the density reaches one-thousandth of its value at the center. At any iteration, the software determines if the system is in the high or partial or non-degenerate regime. It then uses the appropriate approximations to calculate the Fermi-Dirac integrals. In the case of partial degeneracy where no asymptotic behavior is known, the software uses some stored tables that are made by numerically solving the exact form of the Fermi-Dirac integrals. These set of procedures have improved the speed performance of the software, and results are usually returned within a few seconds to a few minutes, depending on the model under study.

5. Study of galaxies

In this section, we would like to use the software to study different DM models. We first validate the software by reproducing two known solutions of the differential equations. Next, we discuss the phase-space bounds on the mass of fermionic DM. A study of non-isothermal dwarf galaxies made of dark particles with the mass of 2 eV is presented in the end.

5.1. Software validation

For validation purposes, we start with an isothermal model with DM mass of 1 MeV at the temperature of 1300 Kelvin, and mass density of $8 \times 10^{-20} \text{kg} \cdot \text{m}^{-3}$ at 1 parsec from the center. The initial parameters are chosen such that the system is in the classical regime where the hydrostatic equation has an exact solution of the form

$$\rho = \frac{k^2 T^2}{2\pi m^2 G} \frac{1}{r^2}. \quad (18)$$

Figure 1 shows the numeric and the exact solutions where the temperature, natural logarithm of the fugacity, and the mass of the galaxy are also presented. The logarithm of the fugacity indicates the classic nature of this model even though a genuine Fermi-Dirac distribution is used. The density has a cusp nature which contradicts observations.

To validate the software in the opposite of the spectrum, we reproduce a fully degenerate DM halo presented in [18] where a lower DM mass limit of 200 eV is derived using the observed line of sight dispersion velocity of dwarf galaxies. We set the DM mass to 200 eV at the temperature of 10^{-4} Kelvin, and mass density of $10^{-20} \text{kg} \cdot \text{m}^{-3}$ at 1 parsec from the center. The profile of

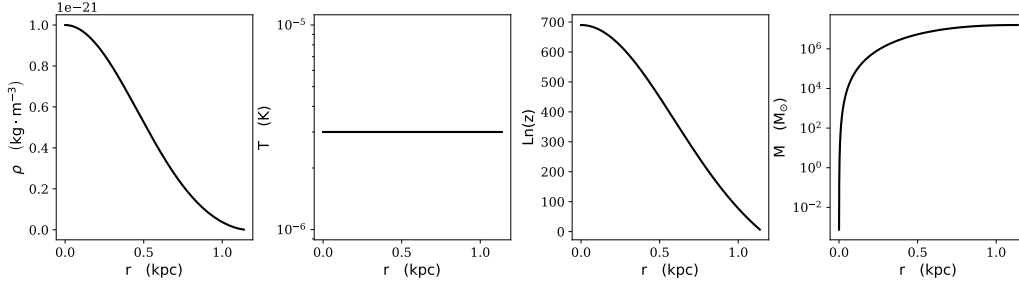


Figure 2: A highly degenerate isothermal DM halo made of 200 eV particles.

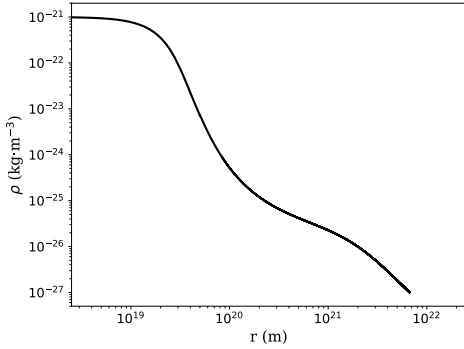


Figure 3: Density profile of a galaxy that is highly degenerate at the center, partially degenerate in the middle and non-degenerate at the edge.

the system is shown in figure 2 where the mass density and total mass of the system are in agreement with those reported in [18]. Since the temperature is not exactly zero, the logarithm of the fugacity is decreasing instead of being infinite as in [18]. Nevertheless, as far as this logarithm is large enough, the full degeneracy regime is valid and the results are stable. This can be understood using the Sommerfeld perturbation of the Fermi-Dirac integrals in Eq. (17).

In the two solutions above, the entire DM halo is either non-degenerate or

highly degenerate. As the last validation, we reproduce the double plateau solution in [26, 27] where DM halo is highly degenerate at the center, partially degenerate in the middle, and non-degenerate close to the edge. To achieve such solution, we choose the mass of DM to be 200 eV, the density at the center to be $\rho_0 = 10^{-21} \text{kg} \cdot \text{m}^{-3}$, and the temperature at the center to be $T_0 = 0.0003$ Kelvin. The solution is depicted in figure 3. It should be noted that, unlike in the previous two solutions, both of the axes are transformed into the logarithmic scales to reproduce the looks of the corresponding solutions in the references.

5.2. Phase-space mass bounds on DM mass

In 1979, Tremaine and Gunn derived the first lower limit on the mass of DM. The derivation depends on a set of assumptions whose validities are not known yet. More specifically they assumed (I) a specific primordial phase-space density, (II) DM is collision-less, i.e., the maximum of its phase-space density is conserved, (III) galactic DM has a Maxwell-Boltzmann distribution, and (IV) DM halo is isothermal. The first two assumptions are not valid for interacting DM. The last two assumptions are also not valid in the degenerate non-isothermal model in which we are interested. The Tremaine-Gunn bound is more related to a knowledge of the primordial phase-space and its evolution over time (which are model dependent) than the Fermi-Dirac statistics of particles. The same bounds apply to some non-fermionic models of dark matter [28].

True models of galactic fermionic DM were later studied in for instance [26, 29, 27]. A lower bound on the mass of a genuinely fermionic DM can be derived using the lower limit of its dispersion velocity at the full degeneracy

level, see for instance [17, 19]

$$\sigma_{\text{F.D}}^2 \geq \sigma_{\text{full-deg.}}^2. \quad (19)$$

If the Maxwell-Boltzmann distribution governs a coarse-grained fermionic DM, its dispersion velocity still needs to be larger than the minimum in Eq. (19), and the inequality leads to a lower limit on the mass of DM. In [18], it is discussed that the inequality is trivial if DM halo is made of a degenerate Fermi gas. In fact, the inequality is trivial as far as the phase-space of DM is the Fermi-Dirac distribution. To see this, we start with the definition of the dispersion velocity

$$\sigma^2 \equiv \frac{kT}{m} h(z), \quad (20)$$

whose minimum is equal to $\frac{1}{5} \left(\frac{3\rho\pi^2 h^3}{m^4} \right)^{\frac{2}{3}}$. Inserting this and the exact equation for the dispersion velocity into Eq. (19) and a straightforward calculation leads to

$$f_{\frac{5}{2}}(z) \geq \frac{6^{\frac{2}{3}} \pi^{\frac{1}{3}}}{10} \left(f_{\frac{3}{2}}(z) \right)^{\frac{5}{3}}. \quad (21)$$

Even in the classical limit where the Fermi-Dirac distribution is effectively Maxwell-Boltzmann, the inequality is trivial. This can be seen by replacing the Fermi-Dirac integrals by their low-fugacity approximation. For this reason, our software exclusively (even in effectively Maxwellian DM halos) works with a Fermi-Dirac distribution such that the limitation of the phase-space is always respected. Although the exclusive use of the Fermi-Dirac distribution for fermionic DM is more robust than other approaches, it does not lift the bound on the mass of fermionic DM. The limitation will express itself when deriving the solutions of the hydrostatic equilibrium, as we will see below.

Recently, fully degenerate models of DM halo have attracted attention mainly due to their potentials for addressing the core-cusp problem [30, 18, 31, 19]. These studies indicate that the lower limit on the mass of DM in a fully degenerate system is of the order of 100 eV which is substantially less than the lower bound that is derived for Maxwellian DM distributions. The studies are, however, focused on isothermal scenarios. In this paper, we would like to investigate non-isothermal but still highly degenerate DM halos. The importance of our study can be shown by first taking a derivative of the mass density in Eq. (9)

$$\frac{d\rho}{d\xi} = \frac{2m(kT_0)^{\frac{3}{2}}}{\alpha^3} \left(\frac{3}{2} y^{\frac{1}{2}} \frac{dy}{d\xi} f_{\frac{3}{2}}(z) + y^{\frac{3}{2}} f_{\frac{1}{2}}(z) \frac{d(\text{Ln}(z))}{d\xi} \right), \quad (22)$$

and then noting that in this equation the temperature gradient $\frac{dy}{d\xi}$ is multiplied by the Fermi-Dirac integral $f_{\frac{3}{2}}(z)$. In a classical system, the Fermi-Dirac integral is close to zero and small departures from an isothermal profile $\frac{dy}{d\xi} = 0$ are negligible. On the contrary, in a highly degenerate system the Fermi-Dirac integral is nearly infinite and small deviations from a constant temperature will be amplified. In the case that the amplified term is dominant, $\frac{dy}{d\xi} = 0$ is an extremely fine-tuned and non-realistic assumption. It is hard to imagine an exactly constant temperature over thousands of light years.

5.3. *Non-isothermal galaxies*

Dwarf satellites are among the densest DM dominated galaxies that are often used to place the most stringent lower limits on the mass of fermionic DM. In this section, we use the observations of dwarf galaxies to investigate the effects of a temperature gradient on the lower mass limits. Our strategy

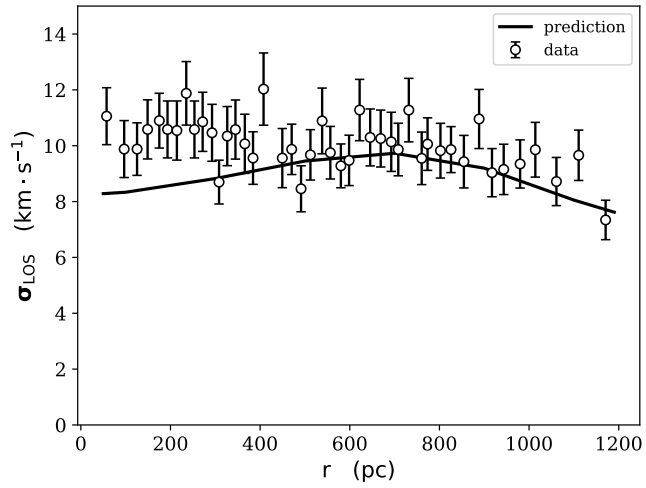


Figure 4: The line of sight dispersion velocity for the Fornax dwarf galaxy of the Milky Way. The solid curve is the best fit line for a linear temperature gradient. The DM mass, and the mass density at the center are fixed before the optimization and are 2 eV and $1.95 \times 10^{-21} \text{ kg} \cdot \text{m}^{-3}$ respectively. The data is from [32].

is to (I) assume a DM mass of 2 eV and a mass density of $1.95 \times 10^{-21} \text{ kg}\cdot\text{m}^{-3}$ at the center, (II) assume a temperature profile of the form $\frac{d^2y}{d\xi^2} = -a$ where a is a positive free parameter, (III) use the data for the line of sight dispersion velocity of the Fornax dwarf satellite of the Milky Way to derive the parameter of the temperature profile as well as the temperature at the center of the galaxy. These are then used as inputs for the software to find the corresponding mass density profile.

The line of sight dispersion velocity is given by [33]

$$\sigma_{\text{LOS}}^{*2}(r) = \frac{2}{I(r)} \int_r^\infty ds \rho^*(s) \sigma^{*2}(s) \frac{s}{\sqrt{s^2 - r^2}}, \quad (23)$$

where asterisk refers to the visible matter and $I(r)$ is a projection profile. Following [32], we choose the Plummer profile

$$\begin{aligned} I(r) &= \frac{3L}{\pi r_{\text{half}}^2} \frac{1}{\left(1 + \frac{r^2}{r_{\text{half}}^2}\right)^2}, \\ \rho^*(r) &= \frac{3L}{4\pi r_{\text{half}}^3} \frac{1}{\left(1 + \frac{r^2}{r_{\text{half}}^2}\right)^{\frac{5}{2}}}, \end{aligned} \quad (24)$$

where L is the luminosity and will be canceled out in the following and r_{half} is the half radius and in the Fornax dwarf galaxy is equal to $\sim 650 \text{ pc}$ [32]. The dispersion velocity of the visible matter can be determined using the equation for the hydrostatic equilibrium

$$\frac{dP^*}{dr} = -G\rho^*(r) \frac{M(r)}{r^2}, \quad (25)$$

where the total mass can be approximated by the mass of DM. Therefore, a simple integration reads

$$\sigma^{*2}(r) = \frac{G}{\rho^*(r)} \int_r^\infty ds \rho^*(s) \frac{M(s)}{s^2}, \quad (26)$$

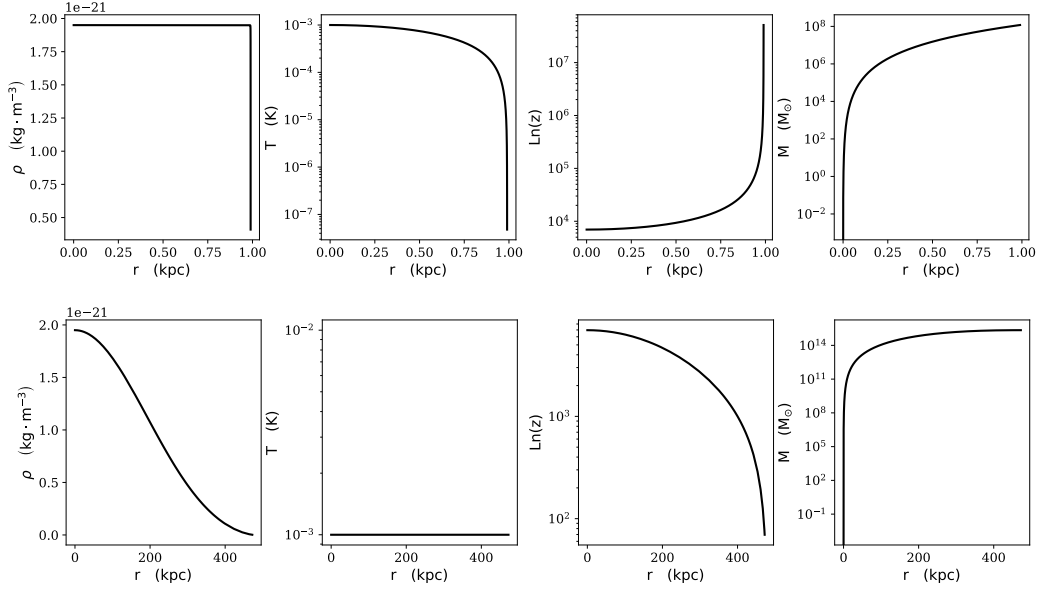


Figure 5: Galactic profile for DM mass of 2 eV and central mass density and temperature of 1.95×10^{-21} kg·m⁻³ and 0.001 Kelvin respectively for (top) temperature profile of $\frac{d^2y}{d\xi^2} = -2.2 \times 10^6$ (bottom) temperature profile of $\frac{d^2y}{d\xi^2} = 0$.

where the visible matter is approximated by a classical ideal gas as in [34] with the EOS of $P^* = \rho^* \frac{kT^*}{m^*} \equiv \rho^* \sigma^{*2}$.

At this point we have all the components for calculating the line of sight dispersion velocity. Using the data for the Fornax dwarf galaxy reported in [32] and using a simple optimization method, we find that $T_0 = 0.01$ Kelvin and $a = 2.2 \times 10^6$ equivalent to a temperature gradient of not more than 0.02 Kelvin per kpc. The data and the best fit line are shown in figure 4. The corresponding profile of the galaxy is shown in figure 5(top). The isothermal profile of the otherwise the same system is shown in figure 5(bottom). The figures indicate that host galaxies like the Milky Way are much larger than compact dwarf galaxies because the two have different temperature profiles.

In an interacting DM model, dwarf galaxies moving through their host, experience a friction that can lead to their needed temperature gradient. The same friction is on the other hand negligible for the host galaxy leading to less (or no) temperature gradient.

Eq. (22) explains why the non-isothermal system does not extend beyond 1 kpc. At around the edge, the temperature is low and fugacity is almost infinite. Therefore, $y^{\frac{1}{2}} \gg y^{\frac{3}{2}}$ and $f_{\frac{3}{2}}(z) \gg f_{\frac{1}{2}}(z)$ which lead to the dominance of the first term over the second term. The sum of the two terms is shown in figure 6 where one can see that the gradient of mass density is extremely large at the edge. The increase in the fugacity of the non-isothermal galaxy can be understood from

$$\text{Ln}(z) = \left(\frac{3\pi^{\frac{1}{2}}\alpha^3\rho}{8m(kT)^{\frac{3}{2}}} \right)^{\frac{2}{3}}, \quad (27)$$

which is obtained after rewriting the mass density in Eq. 9 using the Sommerfeld approximation. The temperature gradient of the dwarf galaxy is shown in figure 7(left). The maximum of the absolute value of the temperature gradient is only 0.002 Kelvin per kpc. Figure 7(right) indicates that DM has higher kinetic energy than the gravitational potential energy at the center. Even though the DM halo is in hydrostatic equilibrium and the net flux of mass is zero, if an imaginary bubble of mass starts to move toward the edge, it loses its kinetic energy to its colder surrounding. Therefore, by the time it arrives at the edge of the galaxy, its kinetic energy has fallen below its gravitational potential energy as can be seen from the figure. The dynamical time for the galaxy is $\sim 10^8$ years. This is the least travel time for the imaginary mass bubble and is long enough to assume that the bubble

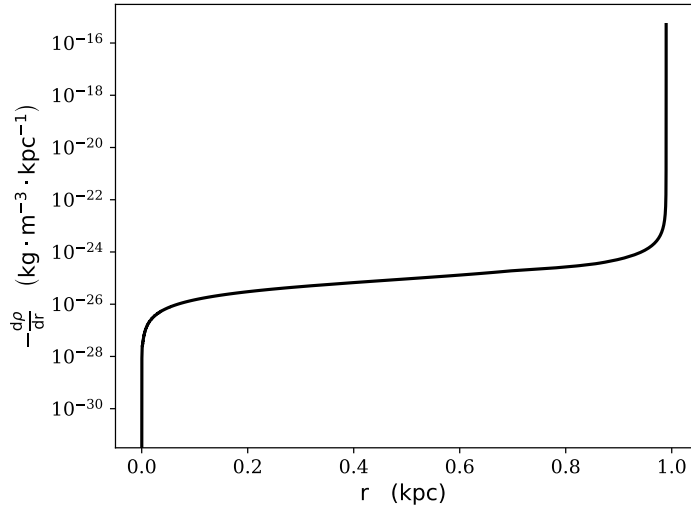


Figure 6: Negative of the gradient of the mass density for a galaxy with DM mass of 2 eV and central mass density of $1.95 \times 10^{-21} \text{ kg}\cdot\text{m}^{-3}$ and central temperature of 0.001 Kelvin with a temperature profile of $\frac{d^2 y}{d\xi^2} = -2.2 \times 10^6$.

always has the same temperature as its surrounding.

6. Sources of heat generation and heat transfer

In the preceding section, we showed that a temperature gradient of not more than one-thousandth of a Kelvin per every 3000 light years could explain the small size of a dwarf galaxy made of DM with the mass of 2 eV. In this section, we show that unlike the equation for hydrostatic equilibrium, the temperature gradient does not have a unique equation. Temperature profiles in galaxies not only depend on the model of DM but also are functions of properties such as relative speeds, the position of other galaxies, and the mass densities. We specifically discuss the means of heat transfer like radiation and convection and the origins of the heat, such as gravitational contraction

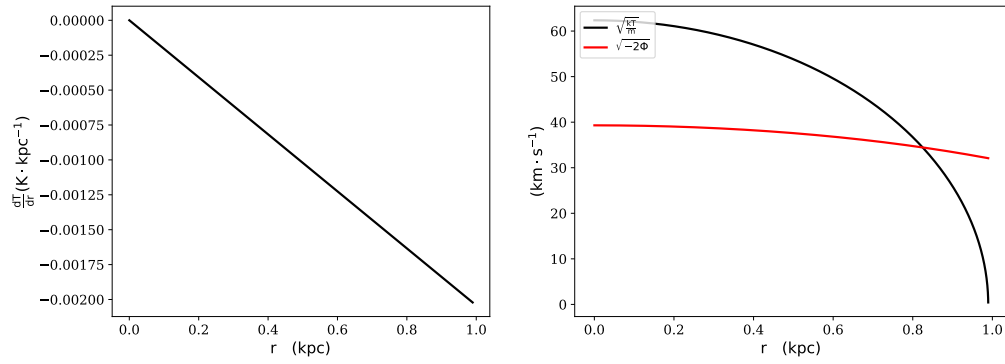


Figure 7: (left) The derivative of the temperature with respect to the distance from the center of the galaxy corresponding to figure 5(top). (right) The red line indicates the escape velocity for the same galaxy. Dark particles at the center have higher kinetic energy than gravitational potential energy. Near the edge, however, their kinetic energy falls toward zero. The dynamical time of the system is roughly 10^8 years. If an imaginary mass bubble moves from the center toward the edge, this extended period assures us that it will lose its kinetic energy to the colder surrounding and cannot escape the system by the time it reached the edge.

and friction.

Friction

Any phenomenon through which the macroscopic kinetic energy of galaxies is transformed, due to the conservation law, to the microscopic kinetic energy of the constituting particles, falls under the category of friction. The drag forces felt by compact dwarf galaxies that are moving through their hosts may set up considerable temperature gradients. Such forces usually depend on the relative speed, the mass densities, and other environmental properties. In collision-less models of DM, the Chandrasekhar friction is the most significant drag force. In interacting models of DM, a variety of frictional forces are possible. For QED-like interactions, the drag force can be approximated by the familiar form of the friction in the fluid dynamics

$$F_{\text{friction}} \propto -\rho v^2, \quad (28)$$

where v is the relative speed. The density dependence of the drag force indicates that the generated heat, equivalent to the work done by the force, is not evenly distributed in the galaxy.

Contraction

Conversion of the gravitational potential energy to the kinetic energy of DM is another mean for heating galaxies. The well-known Kelvin-Helmholtz mechanism belongs to this category. The simplest form of this mechanism is when a single particle that is at rest at the edge of a galaxy falls toward the center. As it moves further inside, its kinetic energy and therefore $\frac{kT}{m}$ increases due to the conservation of energy.

Radiation

In collision-less DM models, only gravitational sources are available for radiation. The Kelvin-Helmholtz mechanism is an example. If DM interacts through a long-range force, in SIDM category, for example, DM can cool down through dark radiations, for instance see [13, 24, 35, 36]. The Eddington equation for temperature gradient due to radiation reads [37]

$$\frac{dT}{dr} = -\kappa \frac{\rho L}{T^3 r^2}, \quad (29)$$

where κ is a constant and L is the luminosity of the radiation at distance r from the center.

Convection

Convection is the most efficient mean of heat transfer and is available to both collision-less and interacting DM models. Since in the literature, the criteria for a system to be convective is mostly derived for ideal classical gases, we discuss convection in Fermi-Dirac systems in more details.

In the following, we first derive a few equations for adiabatic processes and then move to the subject of convection. In a close system, entropy takes the following form $S = S(N, EV^{\frac{2}{3}})$ where E is the total energy. Since the entropy and the number of particles N do not change in adiabatic processes, $EV^{\frac{2}{3}}$ is also a constant in such events regardless of the statistics of the system. On the other hand, the pressure in a close system can be found from $P = -\partial E / \partial V)_{S,N}$ and therefore is proportional to $\rho^{5/3}$. Consequently, a derivative of the adiabatic pressure reads

$$\frac{dP}{dr} = \frac{5P}{3\rho} \frac{d\rho}{dr}. \quad (30)$$

On the other hand, a derivative of Eq. (11) is equal to

$$\frac{dP}{dr} = \frac{P}{T} \frac{dT}{dr} + \frac{kT}{m} \rho \frac{dh}{dr} + \frac{P}{\rho} \frac{d\rho}{dr}, \quad (31)$$

where using $\frac{df_\nu(z)}{dz} = \frac{f_{\nu-1}(z)}{z}$

$$\frac{dh}{dr} = \frac{d(\text{Ln}(z))}{dr} \left(1 - \frac{f_{\frac{5}{2}}(z)f_{\frac{1}{2}}(z)}{\left(f_{\frac{3}{2}}(z)\right)^2} \right). \quad (32)$$

Combining the two gradients of pressure, the temperature gradient in an adiabatic process reads

$$\frac{dT}{dr} = \frac{2T}{5P} \frac{dP}{dr} - \frac{kT^2 \rho}{mP} \frac{dh}{dr}, \quad (33)$$

where the second term is only present in non-classical systems.

Even in hydrostatic equilibrium, mass bubbles are continually moving up and down microscopically. If the displaced bubbles continue their motions for longer distances, the system becomes convective. During the displacement, the density of the mass bubbles changes such that the pressure equilibrium is maintained. Therefore, the mass density of the bubble in the new location reads

$$\mathcal{D}(r \pm \Delta r) = \mathcal{D}(r) \pm \frac{d\mathcal{D}}{dr} \Delta r. \quad (34)$$

In this process the mass density of the surrounding also changes as

$$\rho(r \pm \Delta r) = \rho(r) \pm \frac{d\rho}{dr} \Delta r. \quad (35)$$

The net force on the bubble in the new location is the sum of the gravitational and the Archimedes forces

$$f_{\text{net}} = -\frac{GM(r)}{r^2} \left(\mathcal{D}(r) \pm \frac{d\mathcal{D}}{dr} \Delta r - \rho(r) \mp \frac{d\rho}{dr} \Delta r \right). \quad (36)$$

If the net force is positive(negative) in the outer(inner) location, the bubble continues its motion until it is dissolved and the system becomes convective. Otherwise, the bubble moves back to its original location, and no heat transfer takes place.

The change in the bubble, and not necessarily in the surrounding, is usually fast enough that can be assumed adiabatic. Therefore, using Eq. (30)

$$\frac{d\mathcal{D}}{dr} = \frac{3\rho}{5P} \frac{dP}{dr}, \quad (37)$$

where we have used the fact that the pressure and the initial density of the bubble are always equal to the corresponding ones of the surrounding. Consequently, using Eq. (36), the criteria for the convection reads

$$\frac{d\rho}{dr} - \frac{3\rho}{5P} \frac{dP}{dr} \geq 0. \quad (38)$$

Replacing the first term by its equivalent using Eq. (31) and with a straightforward calculation, the condition for the convection in terms of the temperature gradient reads

$$\frac{dT}{dr} \leq \frac{2T}{5P} \frac{dP}{dr} - \frac{kT^2\rho}{mP} \frac{dh}{dr}. \quad (39)$$

The right hand side is the adiabatic temperature gradient according to Eq. (33). If the heat transfer is fast enough and the galaxy under study is convective, one can take the equality in this equation to determine the temperature gradient in the software rather than directly assuming a temperature profile.

In the end, it should be mentioned that in a convective system, the net flux of mass is zero due to the existence of both incoming and outgoing bubbles. Also, since the incoming bubbles are colder than their surroundings and the outgoing ones are hotter than their surroundings, the heat transfer is effectively outward. More details on convection can be found in the literature.

7. Conclusions and Discussions

We have derived the EOS of a fermionic DM and combined it with the conservation of energy-momentum to find the most general hydrostatic equilibrium equation for spherical halos. Computer software has been developed for the sake of studying the possible solutions of the differential equations. From non-degenerate to highly degenerate Fermi halos with any temperature profile can be investigated with the software. Two known solutions of the equations are reproduced as validations. The effects of small deviations from a constant temperature profile are studied. We have shown that while slight variations in the DM temperature do not lead to significant changes in non-degenerate halos, they can lead to an entirely different mass density profile when the fugacity of DM tends to infinity.

To show that extremely light DM cannot be ruled out by phase-space considerations, we have used the observed line of sight dispersion velocity of the Fornax dwarf galaxy to derive the temperature profile of its DM halo assuming that the DM mass is 2 eV. We assume a linear temperature gradient with one free parameter and use a simple optimization method to find the best fit to the data. With a temperature gradient whose maximum is ~ 0.002 Kelvin per 3000 light years, it is possible to build a halo with the mass of $\sim 10^8 M_\odot$ and the radius of ~ 1 kpc.

Active neutrinos are the least understood part of the SM and neutrino models are still under intense investigations. The predictions of SM in the neutrino sector are at odds with observations, and hot primordial neutrinos are not observed yet. Therefore, it is legitimate to question SM's prediction that active neutrinos freeze-out relativistically in the early universe. We use

the anomalous magnetic moment of electrons as the most precisely tested variable in physics to derive an upper limit on the strength of a new interaction that couples equally to both electrons and neutrinos. We show that the upper limit is a few orders of magnitude higher than the weakest force that is needed to keep neutrinos in thermal contact until they freeze-out cold in the early universe.

In the end, we would like to clarify a few possibly ambiguous points. It may appear that by using the reference frame attached to the center of the galaxy and introducing the gravitational potential energy to the energy of particles in the Fermi-Dirac integrals, and by explicitly expressing the fugacity in terms of the chemical potential, one can remove the temperature dependence of the mass density. The argument goes as follows. In the high degeneracy limit, using the Sommerfeld approximation, the mass density reads

$$\rho = \frac{2mk^{\frac{3}{2}}}{\alpha^3 \Gamma(\frac{5}{2})} T^{\frac{3}{2}} (\text{Ln}(z))^{\frac{3}{2}}. \quad (40)$$

On the other hand, the logarithm of the fugacity is

$$\text{Ln}(z) = \frac{\mu - m\phi}{kT}, \quad (41)$$

where ϕ is the gravitational potential energy in the reference attached to the center of the galaxy, and μ is the chemical potential. Therefore, the two temperatures cancel out and the mass density reads

$$\rho \propto (\mu - m\phi)^{\frac{3}{2}}. \quad (42)$$

At this point, it may seem that the change of variables has removed the temperature dependence of the mass density. This argument is incorrect

because the chemical potential μ is still a non-linear function of temperature. The importance of this temperature dependence is that in non-isothermal galaxies, the derivative of the temperature is not zero. Therefore, a derivative of the mass density reads

$$\frac{\partial \rho}{\partial \xi} \propto [\mu - m\phi]^{\frac{1}{2}} \left(\frac{\partial \mu}{\partial \xi} - m \frac{\partial \phi}{\partial \xi} \right), \quad (43)$$

where the derivative of the chemical potential is a non-isothermal-specific term giving rise to the differences with respect to the isothermal solutions.

Another ambiguity that may arise is that the mass density at $T \simeq 0$ is not a function of temperature because it can be expressed as a function of the Fermi momentum which has no temperature dependence. This argument is also not correct. The mass density in Eq. 9 can be written as

$$\rho \propto \int_0^\infty p^2 dp \frac{1}{\exp\left(\frac{p^2 - \mu}{2m} - \frac{\mu}{kT}\right) + 1}. \quad (44)$$

As the temperature goes to zero, i.e. at $T \simeq 0$, the term in the integrand reads

$$\frac{1}{\exp\left(\frac{p^2 - \mu}{2m} - \frac{\mu}{kT}\right) + 1} \Big|_{T \simeq 0} = \begin{cases} 1, & \frac{p^2}{2m} < \mu|_{T \simeq 0} \\ 0, & \frac{p^2}{2m} > \mu|_{T \simeq 0}. \end{cases} \quad (45)$$

Therefore, at zero temperature,

$$\rho|_{T \simeq 0} \propto \int_0^{\sqrt{2m\mu|_{T \simeq 0}}} p^2 dp = \frac{1}{3} (2m\mu|_{T \simeq 0})^{\frac{3}{2}}, \quad (46)$$

where the chemical potential at zero temperature $\mu|_{T \simeq 0}$ is defined as the Fermi energy $\frac{p_f^2}{2m}$ where p_f is the Fermi momentum. Clearly $\rho|_{T \simeq 0}$ is not a function of temperature. This, however, does not mean that $\left(\frac{\partial \rho}{\partial T}\right)|_{T \simeq 0}$ is

zero. The latter is the term that we have studied in the paper and appears as a non-isothermal-specific term in the differential equations.

Also, one may mistakenly think that it is not possible to compress fermions into extremely small regions because otherwise, the Pauli exclusion principle will be violated. By squeezing the fermions of a container, they will occupy higher momentum levels due to the phase space limitation. Therefore, the pressure on the inner walls of the container will increase. If our force on the outer wall of the box is large enough, we can compress the fermions into arbitrarily small regions. Therefore, it is the stability equation that determines the radius of the box, and a new term in this equation can lead to different container sizes.

Finally, the relationship between the total mass and total radius of DM halo only reads the popular form of $M \sim R^{-3}$ for isothermal highly degenerate halos like the one given by figure 5(bottom). The effect of non-isothermality can be seen in figure 5(top) where M and R do not obey the famous isothermal relation of $M \sim R^{-3}$. The figure indicates that the effect is rather significant. A natural question that may arise is how a negligible temperature gradient can lead to such a significant effect. To answer this, we should note that the temperature gradient in Eq. 22 is multiplied by infinite Fermi-Dirac integrals. In the case of isothermal galaxies, we are assuming that the zero temperature-gradient times the infinite Fermi-Dirac integral is zero, which in some cases can be a fine-tuned assumption.

References

- [1] F. Zwicky, Die Rotverschiebung von extragalaktischen Nebeln, *Helvetica Physica Acta* 6 (1933) 110–127.
- [2] V. C. Rubin, J. Ford, W. K., N. Thonnard, Rotational properties of 21 SC galaxies with a large range of luminosities and radii, from NGC 4605 (R=4kpc) to UGC 2885 (R=122kpc)., *Astrophys. J.* 238 (1980) 471–487. doi:10.1086/158003.
- [3] A. Refregier, Weak Gravitational Lensing by Large-Scale Structure, *Annual Review of Astron and Astrophys* 41 (2003) 645–668. doi:10.1146/annurev.astro.41.111302.102207. arXiv:astro-ph/0307212.
- [4] J. A. Tyson, G. P. Kochanski, I. P. Dell’Antonio, Detailed Mass Map of CL 0024+1654 from Strong Lensing, *Astrophys. J.* 498 (1998) L107–L110. doi:10.1086/311314. arXiv:astro-ph/9801193.
- [5] D. Clowe, M. Bradač, A. H. Gonzalez, M. Markevitch, S. W. Randall, C. Jones, D. Zaritsky, A Direct Empirical Proof of the Existence of Dark Matter, *Astrophys. J.* 648 (2006) L109–L113. doi:10.1086/508162. arXiv:astro-ph/0608407.
- [6] J. L. Weiland, N. Odegard, R. S. Hill, E. Wollack, G. Hinshaw, M. R. Greason, N. Jarosik, L. Page, C. L. Bennett, J. Dunkley, B. Gold, M. Halpern, A. Kogut, E. Komatsu, D. Larson, M. Limon, S. S. Meyer, M. R. Nolta, K. M. Smith, D. N. Spergel, G. S. Tucker, E. L. Wright, Seven-year Wilkinson Microwave Anisotropy Probe (WMAP) Observations: Planets and Celestial Calibration Sources, *Astrophysical*

- Journal, Supplement 192 (2011) 19. doi:10.1088/0067-0049/192/2/19.
arXiv:1001.4731.
- [7] S. W. Allen, R. W. Schmidt, A. C. Fabian, H. Ebeling, Cosmological constraints from the local X-ray luminosity function of the most X-ray-luminous galaxy clusters, MNRAS 342 (2003) 287–298. doi:10.1046/j.1365-8711.2003.06550.x. arXiv:astro-ph/0208394.
- [8] Xenon Collaboration, First Dark Matter Search Results from the XENON1T Experiment, Phys. Rev. Lett. 119 (2017) 181301. doi:10.1103/PhysRevLett.119.181301. arXiv:1705.06655.
- [9] LUX Collaboration, Results from a Search for Dark Matter in the Complete LUX Exposure, Phys. Rev. Lett. 118 (2017) 021303. doi:10.1103/PhysRevLett.118.021303. arXiv:1608.07648.
- [10] PandaX-II Collaboration, Dark matter results from 54-ton-day exposure of pandax-ii experiment, Phys. Rev. Lett. 119 (2017) 181302. URL: <https://link.aps.org/doi/10.1103/PhysRevLett.119.181302>. doi:10.1103/PhysRevLett.119.181302. arXiv:1708.06917.
- [11] A. Boveia, C. Doglioni, Dark Matter Searches at Colliders, Annual Review of Nuclear and Particle Science 68 (2018) 429–459. doi:10.1146/annurev-nucl-101917-021008. arXiv:1810.12238.
- [12] S. F. King, Neutrino mass models, Reports on Progress in Physics 67 (2004) 107–157. doi:10.1088/0034-4885/67/2/R01. arXiv:hep-ph/0310204.

- [13] A. Borzou, Primordial neutrinos: hot in SM-GR- Λ -CDM, cold in SM-LGT, *European Physical Journal C* 78 (2018) 639. doi:10.1140/epjc/s10052-018-6104-6. arXiv:1711.03098.
- [14] D. N. Spergel, P. J. Steinhardt, Observational Evidence for Self-Interacting Cold Dark Matter, *Phys. Rev. Lett.* 84 (2000) 3760–3763. doi:10.1103/PhysRevLett.84.3760. arXiv:astro-ph/9909386.
- [15] S. Tulin, H.-B. Yu, Dark matter self-interactions and small scale structure, *Phys. Rep.* 730 (2018) 1–57. doi:10.1016/j.physrep.2017.11.004. arXiv:1705.02358.
- [16] S. Tremaine, J. E. Gunn, Dynamical role of light neutral leptons in cosmology, *Phys. Rev. Lett.* 42 (1979) 407–410. doi:10.1103/PhysRevLett.42.407.
- [17] A. Boyarsky, O. Ruchayskiy, D. Iakubovskiy, A lower bound on the mass of dark matter particles, *Journal of Cosmology and Astro-Particle Physics* 2009 (2009) 005. doi:10.1088/1475-7516/2009/03/005. arXiv:0808.3902.
- [18] V. Domcke, A. Urbano, Dwarf spheroidal galaxies as degenerate gas of free fermions, *Journal of Cosmology and Astro-Particle Physics* 2015 (2015) 002. doi:10.1088/1475-7516/2015/01/002. arXiv:1409.3167.
- [19] C. Di Paolo, F. Nesti, F. L. Villante, Phase-space mass bound for fermionic dark matter from dwarf spheroidal galaxies, *MNRAS* 475 (2018) 5385–5397. doi:10.1093/mnras/sty091. arXiv:1704.06644.

- [20] N. Kaiser, Constraints on neutrino-dominated cosmologies from large-scale streaming motion, *Astrophys. J.* 273 (1983) L17–L20. doi:10.1086/184121.
- [21] Planck Collaboration, Planck 2015 results. XIII. Cosmological parameters, *Astronomy and Astrophysics* 594 (2016) A13. doi:10.1051/0004-6361/201525830. arXiv:1502.01589.
- [22] T. Aoyama, M. Hayakawa, T. Kinoshita, M. Nio, Tenth-Order QED Contribution to the Electron $g-2$ and an Improved Value of the Fine Structure Constant, *Phys. Rev. Lett.* 109 (2012) 111807. doi:10.1103/PhysRevLett.109.111807. arXiv:1205.5368.
- [23] D. Hanneke, S. Fogwell Hoogerheide, G. Gabrielse, Cavity control of a single-electron quantum cyclotron: Measuring the electron magnetic moment, *Phys. Rev. A* 83 (2011) 052122. doi:10.1103/PhysRevA.83.052122. arXiv:1009.4831.
- [24] M. R. Buckley, J. Zavala, F.-Y. Cyr-Racine, K. Sigurdson, M. Vogelsberger, Scattering, damping, and acoustic oscillations: Simulating the structure of dark matter halos with relativistic force carriers, *Phys. Rev. D* 90 (2014) 043524. doi:10.1103/PhysRevD.90.043524. arXiv:1405.2075.
- [25] Borzou, A., Computer software to study non-isothermal galaxies, 2019. The python code can be found at https://github.com/ahmadborzou/Study_DM_in_Galaxies. It can be run imidiately online at:

https://mybinder.org/v2/gh/ahmadborzou/Study_DM_in_Galaxies-master.git/master. A short video tutorial of the software is available at: https://youtu.be/j4G_38baj_w.

- [26] N. Bilic, G. B. Tupper, R. D. Viollier, Unified description of dark matter at the center and in the halo of the Galaxy, arXiv e-prints (2001) astro-ph/0111366. [arXiv:astro-ph/0111366](https://arxiv.org/abs/astro-ph/0111366).
- [27] H. J. de Vega, P. Salucci, N. G. Sanchez, Observational rotation curves and density profiles versus the Thomas-Fermi galaxy structure theory, MNRAS 442 (2014) 2717–2727. doi:10.1093/mnras/stu972. [arXiv:1309.2290](https://arxiv.org/abs/1309.2290).
- [28] J. J. Dalcanton, C. J. Hogan, Halo Cores and Phase-Space Densities: Observational Constraints on Dark Matter Physics and Structure Formation, Astrophys. J. 561 (2001) 35–45. doi:10.1086/323207. [arXiv:astro-ph/0004381](https://arxiv.org/abs/astro-ph/0004381).
- [29] P.-H. Chavanis, Phase transitions in self-gravitating systems: Self-gravitating fermions and hard-sphere models, Phys. Rev. E 65 (2002) 056123. doi:10.1103/PhysRevE.65.056123. [arXiv:cond-mat/0109294](https://arxiv.org/abs/cond-mat/0109294).
- [30] C. Destri, H. J. de Vega, N. G. Sanchez, Fermionic warm dark matter produces galaxy cores in the observed scales because of quantum mechanics, New Astronomy 22 (2013) 39–50. doi:10.1016/j.newast.2012.12.003. [arXiv:1204.3090](https://arxiv.org/abs/1204.3090).
- [31] L. Randall, J. Scholtz, J. Unwin, Cores in Dwarf Galaxies from Fermi

- Repulsion, MNRAS 467 (2017) 1515–1525. doi:10.1093/mnras/stx161. arXiv:1611.04590.
- [32] M. G. Walker, M. Mateo, E. W. Olszewski, J. Peñarrubia, N. W. Evans, G. Gilmore, A Universal Mass Profile for Dwarf Spheroidal Galaxies?, *Astrophys. J.* 704 (2009) 1274–1287. doi:10.1088/0004-637X/704/2/1274. arXiv:0906.0341.
- [33] J. Binney, S. Tremaine, *Galactic Dynamics: Second Edition*, Princeton University Press, 2008.
- [34] G. A. Mamon, E. L. Łokas, Dark matter in elliptical galaxies - II. Estimating the mass within the virial radius, MNRAS 363 (2005) 705–722. doi:10.1111/j.1365-2966.2005.09400.x. arXiv:astro-ph/0405491.
- [35] C. Boehm, J. A. Schewtschenko, R. J. Wilkinson, C. M. Baugh, S. Pascoli, Using the Milky Way satellites to interactions between cold dark matter and radiation., MNRAS 445 (2014) L31–L35. doi:10.1093/mnrasl/slu115. arXiv:1404.7012.
- [36] T. Binder, M. Gustafsson, A. Kamada, S. M. R. Sandner, M. Wiesner, Reannihilation of self-interacting dark matter, *Phys. Rev. D* 97 (2018) 123004. doi:10.1103/PhysRevD.97.123004. arXiv:1712.01246.
- [37] S. Chandrasekhar, *An introduction to the study of stellar structure*, 1967.